Seismic vulnerability of RC structures: Assessment before and after FRP retrofitting (case study)

C. Desprez, J. Mazars, Panagiotis Kotronis

Seismic Vulnerability of RC Structures: Assessment Before And After FRP Retrofitting (Case Study)

C. Desprez
Université Paris-Est, IFSTTAR, SOA, Paris, France, cedric.desprez@ifsttar.fr

J. Mazars
Grenoble Institute of Technology, Laboratoire 3S-R, Grenoble, France

P. Kotronis
LUNAM Université, Ecole Centrale de Nantes, Gem, CNRS UMR 6183, France

SUMMARY:
In structural engineering, seismic assessment of existing structures is a crucial issue to provide adapted decisions in a vulnerability reduction context. Amongst the widely range of technical solutions for structural upgrading, external reinforcement by Fiber Reinforced Polymer (FRP) is an interesting tool. Nevertheless, the use of FRP as a retrofitting method is limited, one of the reasons being the lack of predictive numerical tools allowing the vulnerability assessment. Based on a case-study, this paper presents a simplified modeling strategy to assess the seismic vulnerability of an existing reinforced concrete building before and after FRP retrofitting. More specifically, the structure is simulated using multifiber beam elements, the model is validated with in-situ ambient vibrations records and a simplified method to consider FRP retrofitting is proposed. Non linear dynamic analysis studies are performed using a synthetic earthquake signal according to the Eurocode 8. Finally, local indicators, based on the European Macroseismic Scale (EMS 98), are adopted to quantify the damage level in the structure, before and after its FRP retrofitting.

Keywords: earthquake; vulnerability; retrofitting; FRP; concrete; multifiber beam.

1 INTRODUCTION

Mitigation of the seismic vulnerability of existing structures is an important issue in earthquake engineering. Amongst the widely range of technical solutions suitable for seismic retrofitting, bonding of Fiber Reinforced Polymer (FRP) is often adopted. In order to help designers, some efficient numerical tools for the seismic assessment of FRP retrofitted structures are needed, able to quantify the structural vulnerability before and after the seismic upgrade. This paper presents a simplified tridimensional non linear dynamic analysis to assess the vulnerability of an existing structure (the Grenoble City Hall). An evaluation is performed before and after it has been numerically upgrade with FRP, following the Eurocode 8 (EC8) prescriptions. The numerical model is mesh taking advantage of multifiber Timoshenko beam elements in the finite element code Cast3m.

2 DESCRIPTION OF THE STRUCTURE

The Grenoble City Hall (GCH) is a reinforced concrete (RC) building, built in 1966. It is composed of two distinct parts, a tower and a peripherical building (Fig. 2.1). Only the tower is studied hereafter. The tower is 52m high, 43m long and 13m large. The upper part is an eleven story frame (Fig. 2.2) supported by a large transfer deck including prestressed concrete beams. The lower part of the tower is composed by a 12m height hall and an underground level. The main structural frame of the tower is made of four RC piers (cores) containing the lift shafts and stairwells.

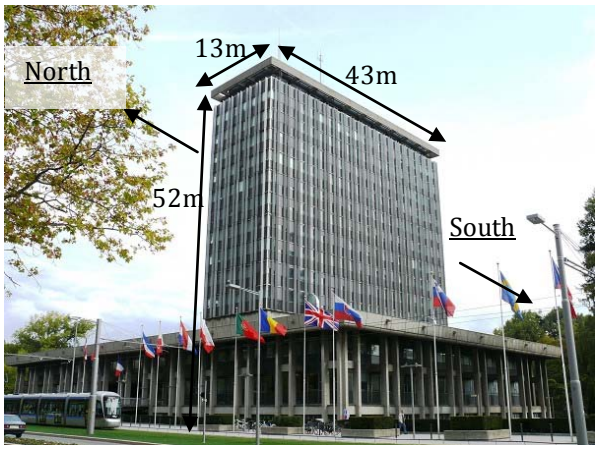

Figure 2.1. CGH - View of the tower and the peripherical building.

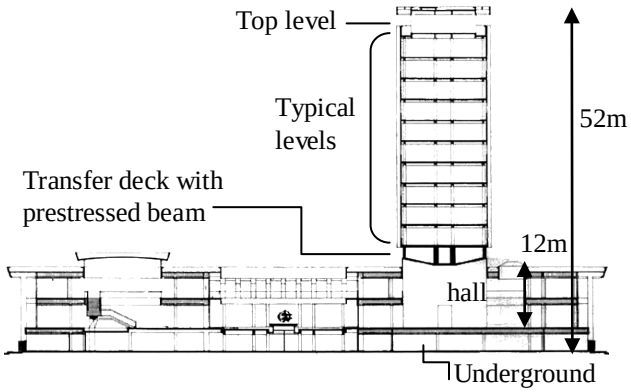

Figure 2.2. GCH - Transverse view of the structure

The structure's ambient vibrations, due to wind, road traffic or small seismic ground motions, are monitored using permanent accelerometers. The response of the structure in terms of accelerations, velocities and displacements is thus known but also its main natural frequencies and possible stiffness evolution (Michel, 2007) (Gueguen et al., 2009).

3 NUMERICAL MODELING

3.1 Modeling strategy

In order to decrease the number of degrees of freedom (DOF) and simplify the finite element mesh, Timoshenko multifiber beam elements are employed for the spatial discretization (Guedes & al., 1994; Kotronis & Mazars, 2005; Mazars & al., 2006; Kotronis, 2008). A structural element is thus simulated using several beams with cross sections divided in fibers (Fig. 3.1). A constitutive model, suitable for cyclic loadings, is associated to each fiber. In the following, shear is considered linear allowing using *1D* non linear constitutive laws. Computations are done with the finite element code Cast3m (Combescure, 2000).

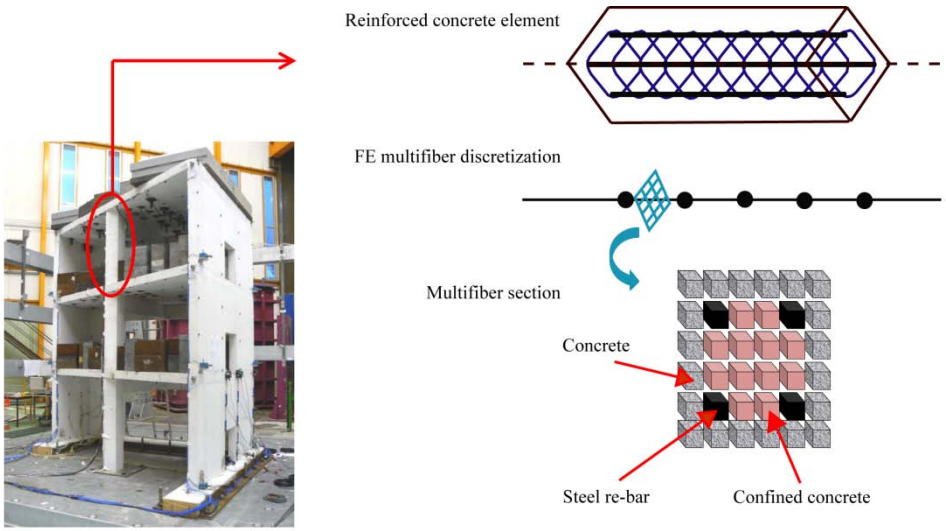

Figure 3.1. Multifiber beam modeling

3.2 Concrete and steel constitutive laws.

The behavior of concrete is described using the constitutive model developed by La Borderie, suitable for cyclic loadings (La Borderie 1991, La Borderie 2003). This one is based on damage mechanics and takes into account the opening and closing of cracks (Fig. 3.2).

The cyclic behavior of steel bars is reproduced using a modified version of the classical Menegotto-Pinto model (Menegotto & Pinto 1973) with cinematic hardening. The model takes into account buckling by introducing a negative modulus slope in compression (Fig. 3.3).

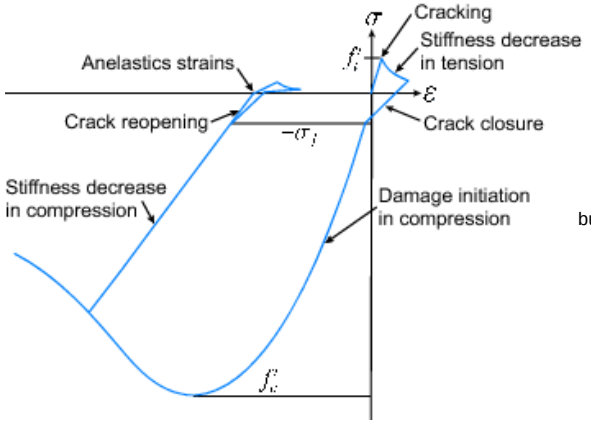

Figure 3.2. La Borderie model - uniaxial stress-strain relation.

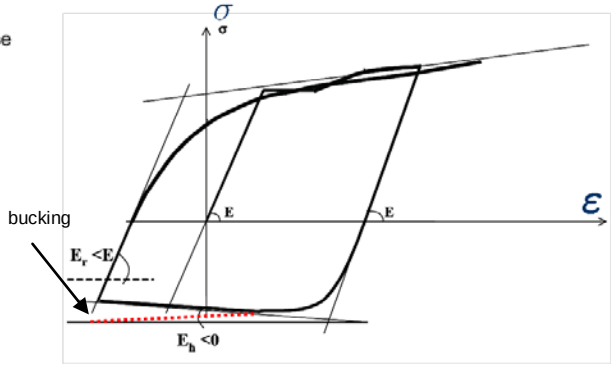

Figure 3.3. Menegoto & Pinto model - uniaxial stress-strain relation.

3.3 Modeling of the structure

Fig. 3.4 shows the finite element mesh of the tower. Non linear multifiber beam elements are used for the piers, beams and columns. All the slabs and the walls at the top level are discretized using linear elastic Kirchhoff plate elements. Linear beam elements are adopted for the prestressed transfer deck. The total number of DOF is 58848. Details about the discretization of the different parts are given in (Desprez, 2010). In order to validate the numerical model, a modal analysis has been performed and the natural frequencies were compared to the ones coming from ambient measurements (Michel, 2007). Up to the fifth frequency, the model correctly matched the in-situ measurements (Fig 3.5) (Michel et al, 2009).

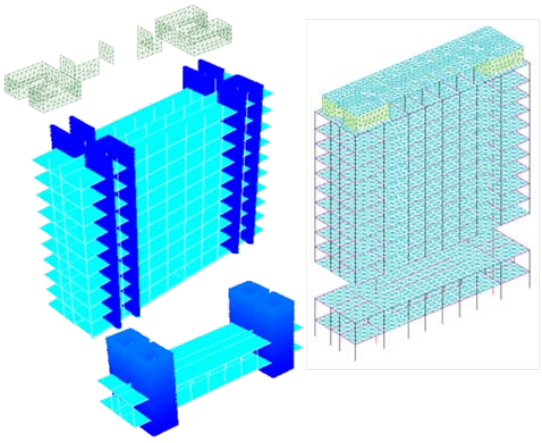

Figure 3.4. CGH – Finite element mesh.

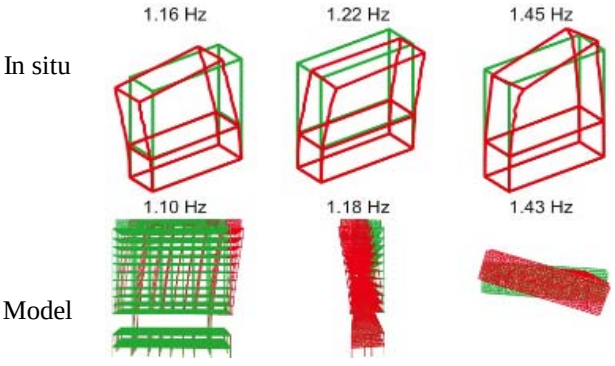

Figure 3.5. GCH – Modal analysis – In-situ records Vs model.

4 VULNERABILITY ASSESSMENT

The dynamic response of the structure is studied in terms of global (displacement, drift) and local (damage, strain) quantities. A synthetic *3D* accelerogram has been used, based on the characteristics of the Grenoble area and EC8 specification (Gueguen, 2009). The peak ground acceleration is close to 3m/s².

4.1 Non linear dynamic analysis

4.1.1 Dynamic behavior

The maximum horizontal top displacements are found equal to 12.3mm and 13.7mm respectively in the longitudinal and transverse direction (Fig. 4.1). Stiffness is visibly higher in the lower part of the tower (rectangular piers) and in the top story (walls). The structure bends mainly according to the first and second flexural modes. The inflexion point is situated just above the transfer deck.
The inter-story drifts are higher in the upper part of the building (Fig. 4.2), evidence of a flexural behavior without important shear effects (the low values at the top floor are due to its wall design). Despite the *3D* loading and the small dissymmetry of the building (differences between the stairwell and the lift shaft cores) no torsion effects are observed.

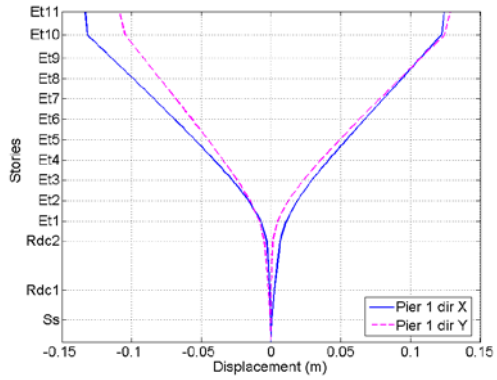

Figure 4.1. GCH - Maximum displacements at the top of one pier: (X) longitudinal and (Y) transverse direction.

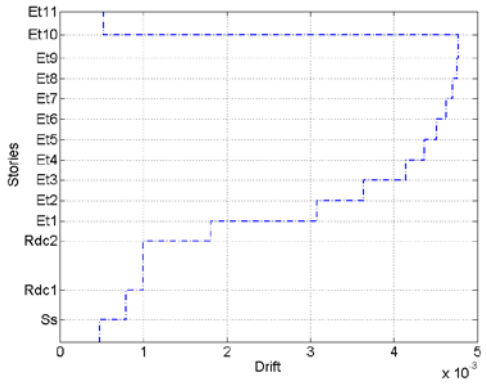

Figure 4.2. GCH - Maximum inter-story drift in one pier: (X) longitudinal and (Y) transverse direction.

4.1.2 Damage distributions

The tensile (D_1) and compressive (D_2) damage variables of the La Borderie model are used to asses the state of the concrete. Although concrete tensile cracking ($D_1 > 0.9$) is not representative of the building capacity, it gives an idea of the areas of the structure where the seismic energy is dissipated. The distribution of the D_1 variable is represented in (Fig. 4.3). Strains are localized at the base of the piers and at the first four levels above the deck.
The High values of the compression damage variable D_2 are representative of concrete spalling and possibility of reinforcement bucking (D_2>0.9). However, during this test, its maximum level only reaches 0.25 at the base of the "U-type" pier.

4.1.3 Strains in steel bars

Fig 4.4 shows the strains envelop in the steel bars of one pier. Two yielding zones are apparent. The first is located at the base of the rectangular pier. The reached value is small, but the location is in a critical part for the stability of the building. The maximum strain value (5.2 10-3) is reached in the first level above the deck. Even if theses yielding values are not excessive, it is important to notice that the building, constructed in the 60s, does not follow the capacity design philosophy.

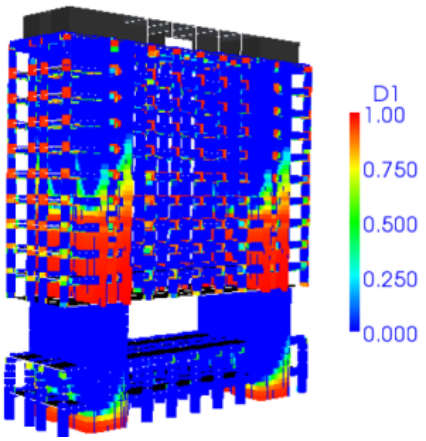

Figure 4.3. GCH – Distribution of D_1 (tension damage).

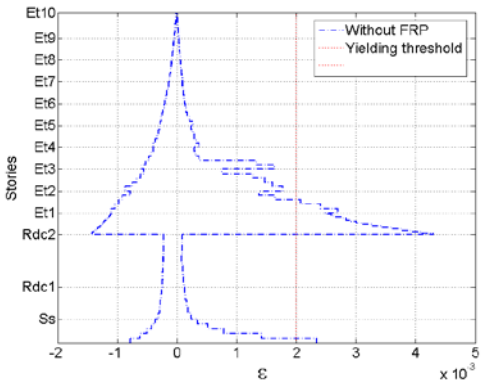

Figure 4.4. GCH – Envelop of strains in the steel bars of pier n°4 (plastic threshold at 0.2%).

4.2 Damage level

The main vulnerability assessment recommendations as Hazus (ATC40, 1996) and Risk-UE LM2 (Risk-UE, 2003) are based on global indicators (respectively the inter-story drift and the top displacement). However, the chosen modeling strategy allows obtaining not only global but also local indicators. For this reason the adopted assessment methodology is based on an equivalence between the European Macro-seismic Scale classification (EMS98, 1998) and local variables as concrete failure and steel bar yielding (Lang, 2002), (Table 4.1).

According to the results of the non linear dynamic analysis, concrete cracking appears at the underground level and at the four first levels above the deck. Reinforcement bars yield at the two first levels above the deck and at the base of the building. No concrete failure due to compression or steel bucking is observed. The damage level is therefore assumed as Moderate (level 2/5).

Table 4.1. Correlation between damage levels (Lang, 2000)

EMS 98	Identification
Negligible to slight damage (no structural damage, slight non-structural damage) Fine cracks in plaster over frame members or in walls at the base. Fine cracks in partitions and infills	point of onset of cracking, => tensile stress at the extreme tensile fibre of the wall section reaches the tensile strength of concrete
Moderate damage (slight structural damage, moderate non-structural damage) Cracks in columns and beams of frames and in structural walls. Cracks in partition and infill walls; fall of brittle cladding and plaster. Falling mortar from the joints of wall panels.	behaviour of the building becomes nonlinear, the stiffness of the building starts to reduce, => yield of the first wall
Substantial to heavy damage (moderate structural damage, heavy non-structural damage) Cracks in columns and beam column joints of frames at the base and at joints of coupled walls. Spalling of concrete cover, buckling of reinforced rods. Large cracks in partition and infill walls, failure of individual infill panels.	increased nonlinear behaviour of the building, the stiffness of the building tends to zero, => yield of the last wall
Very heavy damage (heavy structural damage, very heavy non-structural damage) Large cracks in structural elements with compression failure of concrete and fracture of rebars; bond failure of beam reinforced bars; tilting of columns. Collapse of a few columns or of a single upper floor.	=> ultimate displacement of the first wall, determined either by compression failure of concrete or fracture of the reinforcing bars
Destruction (very heavy structural damage) Collapse of ground floor or parts (e.g. wings) of buildings.	=> drop of the base shear of the building V_b below $2/3 \cdot V_{bm}$

5 FRP RETROFITTING

In order to improve the seismic behavior of the building and to decrease the damage expectance level from Moderate (2/5) to Negligible (1/5) (table 4.1), a FRP retrofitting solution is studied hereafter. According to the previous analysis, the main damage effect is the yielding of reinforced steel bars coming from the flexural bending of the structure, torsion and shear effect being low. The retrofitting strategy consists in upgrading the flexural capacity of the piers by FRP bonding on walls.

5.1 FRP modeling strategy

A simplified methodology to take into account the axial retrofitting for bending elements (beams or walls) is used hereafter. In this particular case, FRP bonded on one side of an element has a function similar to an external reinforcement bar (Figure 5.1). In a finite element model based on multifiber beams, this can be simply reproduced by introducing additional fibers in the beam section (Fig 5.2) with a linear elastic brittle constitutive law (Dufour, 1998; LESSLOSS, 2006; Desprez 2010).

Figure 5.1. Increase of the flexural capacity by FRP bonding on the lower part of a beam.

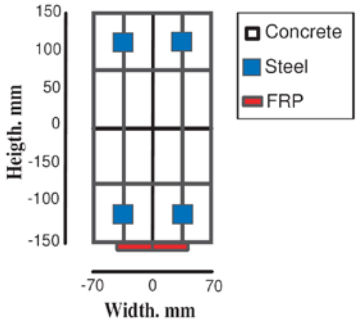

Figure 5.2. Introducing additional FRP fibers in a multifiber beam section.

5.2 Grenoble City Hall retrofitting: design n°1

5.2.1 FRP design n° 1 - Characteristics

The non linear dynamic analysis presented in section 6 highlighted two critical areas. The chosen retrofitted areas are the four main piers, at the underground level and at the four levels above the deck (Fig. 5.3). The thickness of the FRP sheets is calculated to avoid the steel bar yielding. 5mm thick sheets are introduced numerically on the four levels above the deck, and 4mm at the basement level.

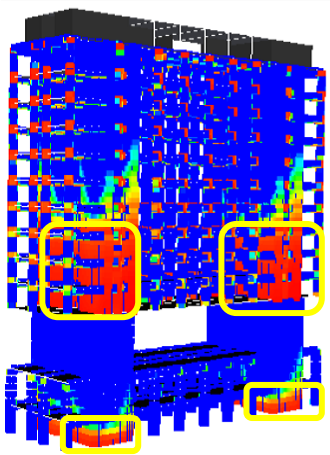

Figure 5.3. GCH (FRP design n°1) - Location of FRP sheets.

5.2.2 Dynamic behavior

Fig. 5.4.a and 5.4.b show that inter-story drifts and floor displacements are higher for the retrofitted than for the non-retrofitted configuration. The use of FRP limits the strains and avoids the creation of plastic hinges inside the reinforced areas (Fig 5.4.c). However, new plastic zones appear just above the retrofitted elements. The discontinuity of the FRP sheets leads to new areas of stain localization in the structure.

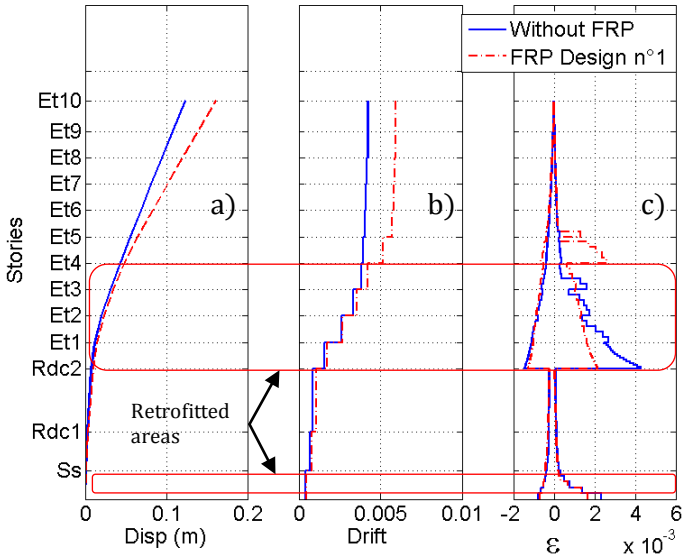

Figure 5.4. GCH (FRP design n°1) - retrofitted Vs non-retrofitted configuration. Response of one pier: (a) displacements, (b) inter-story drifts, (c) steel strains.

5.2.3 Damage distribution

The concrete damage distribution (Fig 5.5) shows an extended area of damage due to tension (D_1) in comparison with the non-retrofitted structure (Fig 4.3). Tensile cracks are important at the base of the tower and above the deck while they reach the fifth level. Damage due to compression is also higher ($D_2 = 0.3$) but still not significant and below the collapse level ($D_2 = 0.9$).

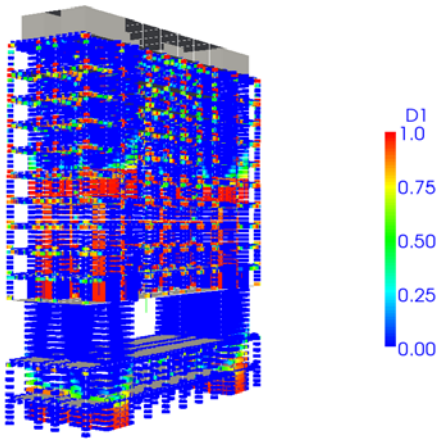

Figure 5.5. GCH – FRP retrofitting - design n°1 - Distribution of D_1 (tension damage).

5.2.4 FRP design n° 1 - Damage assessment

At the final step of the calculation, the structure presents cracks at the base and on the first five levels above the deck. A moderate yielding of the steel bars ($\varepsilon_{max} \approx 2{,}6.10^{-3}$) appears above the retrofitting areas. No concrete compression failure or steel bar buckling is observed. As in section 6, the damage level can thereby be considered moderate (level 2/5). In the following section, an optimized design of the FRP location is studied.

5.3 Grenoble City Hall retrofitting: design optimization

An increase of the FRP sheets is not necessary the best solution to achieve an optimized risk mitigation. It is obvious that the position of plastic hinges is driven by the discontinuities between the retrofitted and the non-retrofitted areas. In the following, the FRP's thicknesses are adjusted considering the internal forces at each level. This leads to a progressive decrease of the FRP thickness of 0,5mm at each level. Furthermore two upper stories (five and six) have been retrofitted to obtain a smoother transition between the retrofitted and the regular parts.

5.3.1 Dynamic behavior and damage location

The maximum top displacement and inter-story drift are similar to the design solution n° 1 (Fig 5.6.a and 5.6.b). Nevertheless, a smoother evolution of the strain localization zone is obtained and the maximum strain values are limited (Fig 5.6.c).

At the end of the loading sequence, the distribution of *D1* shows concentration of strains at the base of the building and on the six levels above the deck (Fig 5.7). The concrete cracks, allowing energy dissipation, are concentrated at the retrofitted areas and no compressive failure is observed.

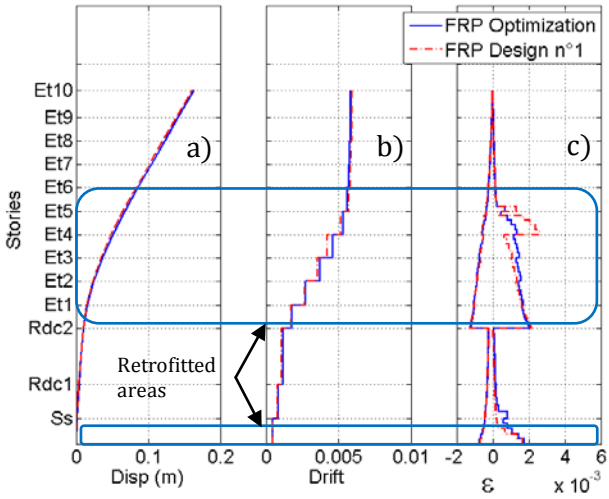

Figure 5.6. GCH - FRP design n°1 retrofitting: retrofitted Vs non-retrofitted configuration. Response of one pier: (a) displacements, (b) inter-story drifts, (c) steel strains.

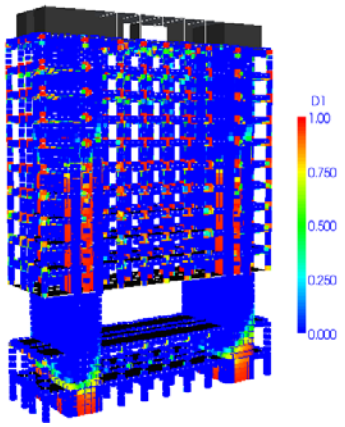

Figure 5.7. GCH (FRP optimization) – Distribution of tension damage (D1), final step.

5.3.2 Damage level

Reinforced bars at the base are not yielded and concrete does not fail due to compression. Applying the methodology of section §4.2 the damage level is now considered Negligible.

6 Conclusions

This paper presents a simplified method to assess the vulnerability of a RC structure before and after its FRP retrofitting. More specifically:

- The structure is simulated using multifiber beam elements and uniaxial constitutive laws for concrete and steel taking into account the cyclic behavior. Comparison between ambient vibrations records and the numerical response proves the good performance of the model. The structure is submitted to a synthetic signal conforming to the EC8 requirements and the results of the non linear dyanamic analysis are presented.
- Local indicators as damage variables and steel strains are used to assess the damage level of the building following the methodology proposed in EMS98 and Lang 2002.
- FRP retrofitting is added to the numerical model and various solutions are studied to decrease the vulnerability level of the structure.

These study highlight the fact that the use of FRP allows reducing the structural damage (local variable) of the building but also induces changes in the flexural behavior. Hence, top displacements and inter story-drifts (global variables) can be found significantly increased. These differences between global and local variables can provide contradictory conclusions depending on the adopted assessment methodologies. Indeed, following the Hazus or Risk-UE specification, a top displacement and interstory-drift enhancement leads to increase the damage level assessment; witch is opposite to the conclusion from the local approach.

It is therefore necessary to adopt concordant indicators. Local variables are most representative of the effective state of a structure, however global indicators are more easy to use after a classical pushover analysis or in-situ measurements. New tools have to be established in order to correctly link the local and global behavior of a structure.

REFERENCES

ATC-40, (1996). Seismic Evaluation and Retrofit of Concrete Buildings, Applied Technology Council.

Combescure D. (2000). Modélisation des structures de génie civil sous chargement sismique à l'aide de Castem 2000, CEA, Direction de l'énergie nucléaire, département modélisation de systèmes et structures, service d'études mécaniques et thermiques, Rapport DM2S.

Desprez C. (2010). Analyse et réduction de la vulnérabilité sismique des structures existantes : renforcement par collage de tissus de fibres de carbone (TFC). PhD, Institut National Polytechnique de Grenoble. (http://tel.archives-ouvertes.fr/tel-00560438/fr/)

Dufour F. (1998). Modélisation du comportement dynamique d'une structure à murs porteurs en béton armé renforcée à l'aide de tissu à fibres de carbone, Master of Science, CEA Saclay, ENS Cachan.

EMS-98. (2001). European Macroseismic Scale 1998, Conseil de l'Europe, Cahiers du centre européen de géodynamique et de séismologie, Vol 19.

Guedes J., Pégon P. and Pinto A. (1994). A fibre Timoshenko beam element in CASTEM 2000, Special publication nr. i.94.31. Technical report, J.R.C, I-21020, European Comission, Ispra, Italy.

Kotronis P. (2000). Cisaillement dynamique de murs en béton armé. Modèles simplifiés 2D et 3D, Thèse de doctorat, Ecole Normale Supérieure de Cachan. (http://tel.archives-ouvertes.fr/tel-00074469/fr/)

Kotronis P. and Mazars J. (2005) Simplified modelling strategies to simulate the dynamic behavior of R/C walls, Journal of Earthquake Engineering ; 9(2):285–306.

Kotronis P. (2008). Stratégies de modélisation de structures en béton soumises à des chargements sévères, Habilitation à diriger des recherches, Université Joseph Fourier, France. (http://tel.archives-ouvertes.fr/tel-00350461/fr/).

La Borderie C. (1991). Phénomènes unilatéraux dans un matériau endommageable: Modélisation et application à l'analyse des structures en béton, Doctoral thesis, Université Paris VI, Paris, France.

La Borderie C. (2003). Stratégies et modèles de calculs pour les structures en béton, Habilitation à diriger des recherches, Université de Pau et des Pays de l'Adour, France.

Lang K. (2002). Seismic vulnérability of existing building. Ph.D , Swiss Federal Institute of Technology, Zurich: s.n.

LESSLOSS, (2006). Integration of knowledge on FRP retrofitted structures, Deliverable 49, Sub-Project 7, Techniques and methods for vulnerability reduction, p 33 - 42.

Mazars J., Kotronis P., Ragueneau F., and Casaux G. (2006). Using multifiber beams to account for shear and torsion: Applications to concrete structural elements. Computer Methods in Applied Mechanics and engineering, 195(52), 7264–7281.

Menegotto M. and Pinto P. (1973). Method of analysis of cyclically loaded reinforced concrete plane frames including changes in geometry and non-elastic behaviour of elements under combined normal force and bending. IABSE Symposium on resistance and ultimate deformability of structures acted on by well-defined repeated loads, final report, Lisbon.

Michel C. (2007). Vulnérabilité sismique de l'échelle du bâtiment à celle de la ville, PhD, Laboratoire de Geophysique Interne et Techtonophysique (LGIT), Université Joseph Fourier, Grenoble I. 2007.

Michel C., Guéguen, P., El Arem, S., Mazars, J., Kotronis, P. (2009). Full-scale dynamic response of an RC building under weak seismic motions using earthquake recordings, ambient vibrations and modelling, Vol 39, n° 4, p 419 - 441, DOI 10.1002/eqe.948.

RISK-UE, (2003). An advance approache to earthquake risk scenarios with applications to different European towns.